Interband and intraband effects in the upper critical field of disordered MgB_2

P. Brotto,[1] I. Pallecchi,[2] M. Putti,[1,2] and E. Galleani D'Agliano[1,2]
[1]*Universitá degli Studi di Genova, via Dodecaneso 33, 16146 Genova, Italy*
[2]*CNR-SPIN, Corso Perrone 24, 16152 Genova, Italy*
(Received 26 July 2010; published 8 October 2010)

In this work the superconducting properties of disordered MgB_2 in applied magnetic field are studied within the $\lambda^{\theta\theta}$ model, by taking into account the presence of both *interband* and *intraband* scattering with impurities. This approach allows to extract the suppression of the critical temperature T_c and the enhancement of the upper critical field H_{c_2}, as a consequence of the introduction of impurities in the samples. We analyze the dependence of H_{c_2} on temperature, anisotropy of the electronic structure, and intraband σ and π band scattering rates. Comparing our numerical calculations with experimental data on irradiated samples, we find that irradiation defects mainly affect the mobility of σ carriers. These results rationalize why the H_{c_2} anisotropy of irradiated samples is quickly reduced with increasing doses and full suppression of superconductivity occurs at rather low-resistivity values. Moreover, our calculations point out that disorder in the π bands affects only weakly the coupling constants and thus it could yield a significant enhancement of H_{c_2} without severe suppression of T_c.

DOI: 10.1103/PhysRevB.82.134512 PACS number(s): 74.70.Ad, 74.25.Op, 74.62.En

I. INTRODUCTION

The discovery of superconductivity in MgB_2 (Ref. 1) provoked a great excitement in the scientific community as a consequence of its peculiar and remarkable properties. It becomes superconducting at 39 K (which is a surprisingly high value if compared with other intermetallic compounds), it is notably simple in composition and structure and conventional electron-phonon mechanism gives rise to superconductivity. Moreover one of the most interesting aspects of the physics of MgB_2 resides in the multigap character of its superconductivity. This feature which had been theoretically predicted in 1959,[2] found its paradigm in MgB_2, which is characterized by the presence of two distinct energy gaps which open in the σ and π sheets of the Fermi surface and by weak interband scattering which does not average the characteristics of each band.

The simple structure of MgB_2 and the conventional character of its coupling mechanism allow for an accurate and reliable description of its physical parameters by detailed *ab initio* calculations. Considering its unique characteristics, a further and deeper investigation of the rich physics which characterizes this material has been strongly encouraged since its discovery.

In this respect, a special attention has been given to the effects of impurities. In fact in the presence of disorder a peculiar behavior is expected for multigap superconductors, where the scattering with impurities involves electrons of different bands, with different characteristics, which gives origin to a great variety of physical phenomena that are not observed in isotropic single-gap materials. Moreover a selective introduction of impurities which differently affect the two bands can effectively tune the superconducting parameters of MgB_2, whose properties can be significantly improved.

This is the case of the upper critical field, H_{c_2}, whose peculiar behavior can be explained only within a two-band model. Indeed H_{c_2}, in comparison with single-gap superconductors, exhibits large values and upward curvatures close to T_c, does not scale with the resistivity in dirty samples, and its anisotropy in different samples can be an increasing or decreasing function of temperature.[3–9] These aspects have been extensively investigated theoretically[10–13] showing how the occurrence of different scattering rates in the two bands can explain many of the observed features. These models evidence that in disordered samples interband scattering is no more negligible and causes a reduction in T_c down to a saturation value but they do not take into account the role of intraband scattering in suppressing T_c. In experimental data of disordered MgB_2, T_c, far from saturating, is completely suppressed at rather low levels of disorder [residual resistivity values on the order of 80 $\mu\Omega$ cm, which roughly correspond to a scattering rate of 0.6 eV (Ref. 14)] and this can be well explained by a smearing of the partial density of states (PDOS) caused by intraband scattering mechanisms.[15] Two bands play a role also in this context: indeed the partial DOS of σ band N_σ is more affected by scattering mechanisms than the partial DOS of π band N_π because it vanishes at 0.7 eV above the Fermi energy and it can be significantly reduced if the smearing involves states above this value. This further asymmetry between σ and π bands can strongly affect the superconducting properties of disordered samples. All these aspects should be carefully considered for a complete understanding of the H_{c_2} behavior.

In this paper we further extend the zero-field analysis of Ref. 15 by studying H_{c_2} of MgB_2 in the presence of disorder within the $\lambda^{\theta\theta}$ model. Both the effects of *interband* and *intraband* scattering mechanisms in suppressing T_c are taken into account. This allows for a self-consistent comparison with experimental data in which interband and π and σ intraband scattering rates are simultaneously determined. The analysis of the upper critical field of irradiated samples shows that irradiation produces defects which mainly affect the mobility of σ band carriers. This result makes it clear why suppression of superconductivity occurs at rather low-resistivity values.

II. THEORY

Following Mansor and Carbotte[12] the strong-coupling linearized gap equations for a multiband system in the presence of an external magnetic field, which determine the upper critical field H_{c_2}, are

$$\tilde{\Delta}_i(n) = \pi T \sum_{m,j} \left\{ [\lambda_{ij}(m-n) - \mu^*_{ij}] + \delta_{mn}\left(\frac{1}{2\pi T}\right)\gamma_{ij} \right\} \chi_j(m)\tilde{\Delta}_j(m), \quad (1)$$

$$\tilde{\omega}_i(n) = \omega_n + \pi T \sum_{m,j} \left[\lambda_{ij}(m-n) + \delta_{mn}\left(\frac{1}{2\pi T}\right)\gamma_{ij} \right] \mathrm{sgn}\, \tilde{\omega}(m) \quad (2)$$

with

$$\chi_i(n) = \frac{2}{\sqrt{\alpha_i \kappa_i}} \int_0^\infty dq e^{-q^2} \tan^{-1}\left(\frac{q\sqrt{\alpha_i\kappa_i}}{|\tilde{\omega}_i(n)|}\right), \quad (3)$$

where the dependence on the magnetic field is contained in the variables α_i defined as follows:

$$\alpha_i = \frac{e}{2} H_{c_2}(T)(v^{ab}_{F_i})^2. \quad (4)$$

In the above equations, $v^{ab}_{F_i}$ are the Fermi velocities on the ab plane for each band, ω_n the Matsubara electron frequencies, λ_{ij} the electron-phonon coupling parameters, μ^*_{ij} the Coulomb pseudopotential, and γ_{ij} the matrix elements relative to the scattering rate with impurities.

The parameter κ_i in Eq. (3) is the ith band anisotropic effective-mass parameter (see Ref. 16) which contains the dependence on the orientation of the applied field with respect to the crystal axes. Assuming, as it is usually done for MgB_2, an isotropic π band structure and a quasi-two-dimensional σ band structure, we have

$$\kappa_\pi = 1,$$

$$\kappa_\sigma(\vartheta) = \sqrt{\cos^2(\vartheta) + \mu \sin^2(\vartheta)},$$

where ϑ is the angle between the applied field and the c axis, and $\mu = \frac{m^{ab}_\sigma}{m^c_\sigma}$ is the ratio between the ab-plane and the c-direction σ band masses.

In order to put Eqs. (1) and (2) in a simpler form which allows to obtain, in some cases, the analytic expression for the critical field, we introduce two approximations. First of all we ignore retardation effects and use the "two-square-well" approximation ($\lambda^{\theta\theta}$ model, see, e.g., Ref. 17), which allows to put the equations in a BCS-type form. The applicability and accuracy of the results that can be obtained in this model have been already verified in the calculations of the critical temperature in disordered MgB_2 samples in the absence of magnetic field.[15] Moreover we focus our attention on systems with high level of impurities and then we assume that both bands are in the dirty limit. In the case of MgB_2 the definition of the dirty limit must be considered separately for each conduction band, which means that the coherence length of the ith band (ξ_i) should be much larger than the mean-free path of the same band ($\xi_i \gg l_i$). In ordinary MgB_2 samples, in the π band, as a consequence of its very large coherence length ξ_π, the condition for the dirty limit ($\xi_\pi \gg l_\pi$) is usually fulfilled while the σ band in usually in the clean limit. In our model we require that both bands are in the dirty limit; this condition can be satisfied when disorder is artificially introduced in the system, as in the case of irradiated samples.

The Eliashberg equations for the energy gap of a multiband superconductor within the two-square-well approximation are the following:

$$\tilde{\Delta}_i(n) = \pi T \sum_j (\lambda_{ij} - \mu^*_{ij}) \sum_{|\omega_m|<\omega_c} \chi_j(m)\tilde{\Delta}_j(m) + \frac{1}{2}\sum_j \gamma_{ij}\chi_j(n)\tilde{\Delta}_j(n),$$

$$\tilde{\omega}_i(n) = \omega_n\left[1 + \sum_j \lambda_{ij}\right] + \frac{1}{2}\sum_j \gamma_{ij}\, \mathrm{sgn}\, \omega_n. \quad (5)$$

Here $\lambda_{ij}(m-n) = \lambda_{ij}\vartheta(|\omega_m| < \omega_c)\vartheta(|\omega_n| < \omega_c)$ and ω_c is a characteristic cut-off frequency.

Equation (5) can be written in the matrix form

$$\left[[\hat{\chi}(n)]^{-1} - \frac{\hat{\Gamma}}{2}\right]\hat{\chi}(n)\bar{\mathbf{\Delta}}(n) = \bar{\mathbf{\Delta}}, \quad (6)$$

where we have defined

$$\bar{\mathbf{\Delta}} = \hat{\Lambda}\pi T \sum_{|\omega_m|<\omega_c} \hat{\chi}(m)\bar{\mathbf{\Delta}}(m) \quad (7)$$

with

$$\hat{\Lambda} = \hat{\lambda} - \hat{\mu}^*,$$

$$\hat{\chi} = \chi_i\delta_{ij},$$

$$\hat{\Gamma} = \begin{pmatrix} \gamma_{\sigma\sigma} & \gamma_{\sigma\pi} \\ \gamma_{\pi\sigma} & \gamma_{\pi\pi} \end{pmatrix}, \quad (8)$$

where the matrices $\hat{\lambda}$ and $\hat{\mu}^*$ are defined as

$$\hat{\lambda} = \begin{pmatrix} \lambda_{\sigma\sigma} & \lambda_{\sigma\pi} \\ \lambda_{\pi\sigma} & \lambda_{\pi\pi} \end{pmatrix} = \begin{pmatrix} \lambda_{\sigma\sigma}(0)\frac{N_\sigma(\gamma_{\sigma\sigma})}{N_\sigma(0)} & \lambda_{\sigma\pi}(0)\frac{N_\pi(\gamma_{\pi\pi})}{N_\pi(0)} \\ \lambda_{\pi\sigma}(0)\frac{N_\sigma(\gamma_{\sigma\sigma})}{N_\sigma(0)} & \lambda_{\pi\pi}(0)\frac{N_\pi(\gamma_{\pi\pi})}{N_\pi(0)} \end{pmatrix},$$

$$\hat{\mu}^* = \begin{pmatrix} \mu^*_{\sigma\sigma} & \mu^*_{\sigma\pi} \\ \mu^*_{\pi\sigma} & \mu^*_{\pi\pi} \end{pmatrix} = \mu^{(0)} \times \begin{pmatrix} 2.23\frac{N_\sigma(\gamma_{\sigma\sigma}) + N_\pi(\gamma_{\pi\pi})}{N_\sigma(\gamma_{\sigma\sigma})} & \frac{N_\sigma(\gamma_{\sigma\sigma}) + N_\pi(\gamma_{\pi\pi})}{N_\sigma(\gamma_{\sigma\sigma})} \\ \frac{N_\sigma(\gamma_{\sigma\sigma}) + N_\pi(\gamma_{\pi\pi})}{N_\pi(\gamma_{\pi\pi})} & 2.48\frac{N_\sigma(\gamma_{\sigma\sigma}) + N_\pi(\gamma_{\pi\pi})}{N_\pi(\gamma_{\pi\pi})} \end{pmatrix}, \quad (9)$$

where the values of the coupling parameters $\lambda_{ij}(0)$ have been taken from the first-principles calculations available in literature[18] $\lambda_{\sigma\sigma}(0)=1.017$, $\lambda_{\sigma\pi}(0)=0.213$, $\lambda_{\pi\sigma}(0)=0.155$, and $\lambda_{\pi\pi}(0)=0.448$, and the scaling law for the pseudopotential has been assumed according to Ref. 19, with $\mu^{(0)}=0.0503$.

Following Ref. 15 we take account of the effect of intraband scattering rates assuming that both $\hat{\lambda}$ and $\widehat{\mu^*}$ depends also on the values of $\gamma_{\sigma\sigma}$ and $\gamma_{\pi\pi}$ via the PDOS N_σ and N_π.

From Eqs. (6) and (7) and the definitions in Eqs. (8) and (9) we obtain an equation for the new gap $\bar{\boldsymbol{\Delta}}$,

$$\bar{\boldsymbol{\Delta}} = \hat{\Lambda}\pi T \sum_m [\hat{A}(m)]^{-1}\bar{\boldsymbol{\Delta}}, \tag{10}$$

where the matrix $\hat{A}(n)$ is defined as

$$\hat{A}(n) = \left[[\hat{\chi}(n)]^{-1} - \frac{\hat{\Gamma}}{2} \right]. \tag{11}$$

Another approximation can be introduced considering the level of disorder present in the system. In fact when both bands are in the dirty limit the inverse tangent in Eq. (3) can be expanded and we obtain the following expression for the quantity $\chi_i(n)$:

$$[\chi_i(n)]^{-1} \cong |\tilde{\omega}_i(n)| + \frac{\alpha_i}{3|\tilde{\omega}_i(n)|}. \tag{12}$$

Also, the second of Eq. (5), in the dirty limit, can be approximated in the following way:

$$|\tilde{\omega}_i(n)| \cong \frac{1}{2}\sum_j \gamma_{ij}$$

and this can be used in the second term of Eq. (12) where

$$\frac{\alpha_i}{3|\tilde{\omega}(n)|} \cong \frac{\alpha_i}{3/2(\gamma_{ii}+\gamma_{ij})}.$$

This yields the following expression for $\hat{A}(n)$:

$$\hat{A}(n) \cong \begin{pmatrix} |\tilde{\omega}_\sigma^{(0)}| + \dfrac{\kappa_\sigma \alpha_\sigma}{3/2(\gamma_{\sigma\sigma}+\gamma_{\sigma\pi})} + \dfrac{\gamma_{\sigma\pi}}{2} & -\dfrac{\gamma_{\sigma\pi}}{2} \\ -\dfrac{\gamma_{\pi\sigma}}{2} & |\tilde{\omega}_\pi^{(0)}| + \dfrac{\alpha_\pi}{3/2(\gamma_{\pi\sigma}+\gamma_{\pi\pi})} + \dfrac{\gamma_{\pi\sigma}}{2} \end{pmatrix} \tag{13}$$

with

$$|\tilde{\omega}_i^{(0)}| = |\omega_n|(1+\lambda_{ii}+\lambda_{ij}).$$

In order to reduce the number of free parameters, we assume a linear relationship between the total scattering rate $\gamma_{\rm tot} \simeq \gamma_{\sigma\sigma}+\gamma_{\pi\pi}$ and the $\sigma\pi$ interband scattering rate $\gamma_{\sigma\pi}=a\gamma_{\rm tot}$, where the constant can be evaluated from the analysis of the zero-field critical temperature T_c as a function of resistivity (for details about this procedure see Ref. 15). Thus, we can obtain from the gap Eq. (10) the value of the upper critical field as a function of a minimal set of parameters (see the Appendix for details),

$$H_{c_2} \equiv H_{c_2}\left[T, \gamma_{\rm tot}, \frac{\gamma_{\sigma\sigma}}{\gamma_{\pi\pi}}, \beta(\vartheta) \right]. \tag{14}$$

Here, the dependence on the different characteristics of the two bands and on the orientation of the applied field is contained in a single parameter $\beta(\vartheta)$ defined as

$$\beta(\vartheta) = \frac{\kappa_\sigma(\vartheta)\alpha_\sigma}{\alpha_\pi} = \frac{(v_{F_\sigma}^{ab})^2}{(v_{F_\pi}^{ab})^2}\kappa_\sigma(\vartheta). \tag{15}$$

From a numerical analysis of the solutions of Eq. (10) we can study the behavior of the critical field varying the four variables which appear in Eq. (14).

In order to understand the role played by each of these quantities, in the following we present the results of the numerical calculations of the upper critical field at $T=0$ K $[H_{c_2}(0)]$, obtained assigning two typical values to one of the parameters in Eq. (14) and varying the two remaining parameters within a realistic range.

It is worth noting that each point of the surfaces reported in the graphs presented in the next sections corresponds to a different T_c value; indeed T_c, like $H_{c_2}(0)$, depends both on $\gamma_{\rm tot}$, through the interband scattering rate, and on $\frac{\gamma_{\sigma\sigma}}{\gamma_{\pi\pi}}$, because of the smearing of the partial DOS.[15] This will be discussed later in comparison with experimental data.

III. THEORETICAL RESULTS

A. $H_{c_2}(0)$ versus β, $\gamma_{\rm tot}$, and $\frac{\gamma_{\sigma\sigma}}{\gamma_{\pi\pi}}$

In the graphs [Figs. 1(a) and 1(b)] we show how the dependence of $H_{c_2}(0)$ on the total scattering rate $\gamma_{\rm tot}$ and on the ratio between the intraband scattering rates $\frac{\gamma_{\sigma\sigma}}{\gamma_{\pi\pi}}$ can be strongly modified by the value of β. We consider the cases of field parallel to the ab plane $[\beta(\frac{\pi}{2})=\frac{(v_{F_\sigma}^{ab})^2}{(v_{F_\pi}^{ab})^2}\sqrt{\frac{m_\sigma}{M_\sigma}}\cong 0.1]$ and perpendicular to the ab plane $[\beta(0)=\frac{(v_{F_\sigma}^{ab})^2}{(v_{F_\pi}^{ab})^2}\cong 0.7]$ (the values of

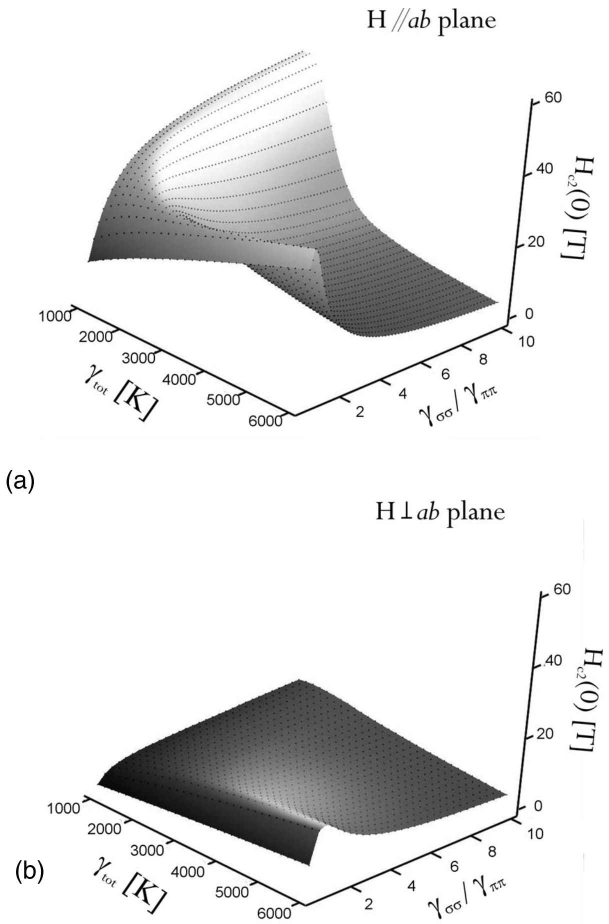

FIG. 1. H_{c_2} as a function of $\gamma_{\rm tot}$ and $\frac{\gamma_{\sigma\sigma}}{\gamma_{\pi\pi}}$ for: (a) field parallel to the *ab* plane—$\beta(\vartheta)\cong 0.1$ and (b) field perpendicular to the *ab* plane—$\beta(\vartheta)\cong 0.7$.

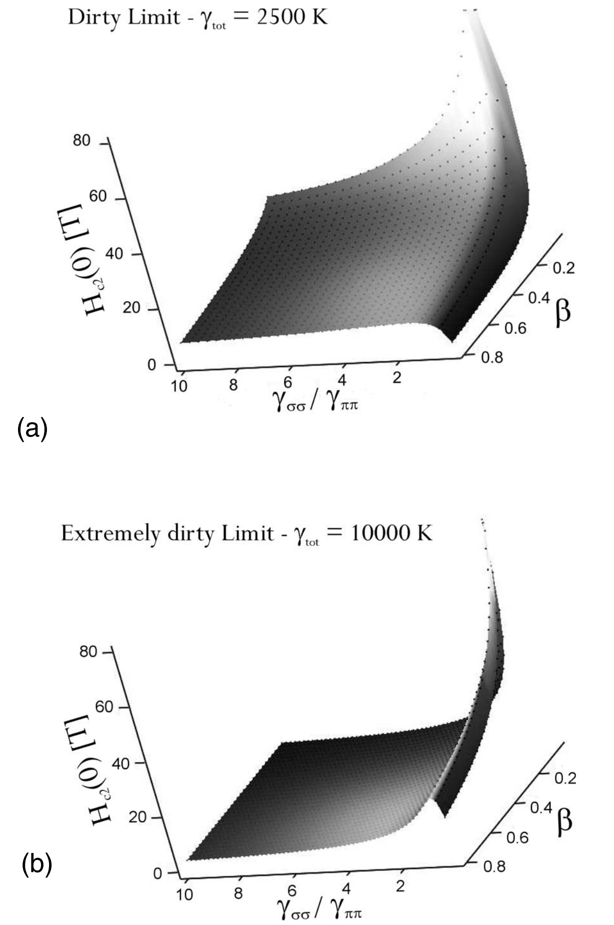

FIG. 2. H_{c_2} as a function of $\frac{\gamma_{\sigma\sigma}}{\gamma_{\pi\pi}}$ and β for: (a) dirty limit case—$\gamma_{\rm tot}$=2500 K and (b) extremely dirty limit case—$\gamma_{\rm tot}$ =10 000 K.

σ and π band Fermi velocities are taken from the first-principles calculations of Ref. 20).

For β=0.1 [Fig. 1(a)] the surface shows a maximum which shifts to higher values of $\gamma_{\rm tot}$ as the ratio $\frac{\gamma_{\sigma\sigma}}{\gamma_{\pi\pi}}$ decreases. For β=0.7 [Fig. 1(b)] the first maximum disappears while the second one is lowered but can still be observed.

These results reproduce the experimental observations which show that the critical field is higher when the field is parallel to the *ab* plane. Moreover an increase in the value of β can also be interpreted as a reduction in the electronic-structure anisotropy which disappears for β=1, i.e., for the totally isotropic case (fully isotropic bands and equal values for the Fermi velocities in σ and π bands). The flattening of the surface when β is increased entails a lower effect of impurities on the critical field of isotropic materials.

As well known, the interband impurity scattering reduces the anisotropic character of the system and yields a crossover from two-gap to single-gap behavior, as observed in irradiated samples with critical temperature value below 10 K (Ref. 21) and estimated total scattering rate over 10 000 K.[15]

In Fig. 2(a) we report the case of the two-gap behavior ($\gamma_{\rm tot}$=2500 K and $\gamma_{\sigma\pi}$=150 K$\ll\theta_D\simeq$600 K) and that of single-gap behavior ($\gamma_{\rm tot}$=10 000 K and $\gamma_{\sigma\pi}$=600 K$\sim\theta_D$).

Looking at the two graphs it is possible to notice that when the level of disorder introduced in the system is low enough to preserve the multigap behavior [Fig. 2(a)] there is a significant $H_{c_2}(0)$ dependence on β for all the values of $\frac{\gamma_{\sigma\sigma}}{\gamma_{\pi\pi}}$ but steeper when $\gamma_{\sigma\sigma}<\gamma_{\pi\pi}$. In the region of single-gap behavior [Fig. 2(b)] the sharp maximum, which appears in the surface when the field is parallel to the *ab* plane ($\beta\approx 0.1$) and $\gamma_{\sigma\sigma}\leq\gamma_{\pi\pi}$, can still be observed while the value of $H_{c_2}(0)$ is nearly constant along the β axis for $\gamma_{\sigma\sigma}>\gamma_{\pi\pi}$. These results make clear how in MgB_2 the effects of the anisotropy on H_{c_2} are due to both the multiband characteristics, which disappears in highly disordered systems as a consequence of interband scattering with impurities, and to the quasi-two-dimensional character of the σ band, which tends to survive when the disorder is introduced mainly in the π band.

In Fig. 3(a) we show the dependence of $H_{c_2}(0)$ on $\gamma_{\rm tot}$ and β when the intraband scattering rate is higher in σ band than in π band ($\gamma_{\sigma\sigma}>\gamma_{\pi\pi}$) while in Fig. 3(b) we consider the opposite situation of π band dirtier than σ band ($\gamma_{\pi\pi}>\gamma_{\sigma\sigma}$). In the first case a pronounced maximum appears for low β values and $\gamma_{\rm tot}$ around 2000 K. In the second case we can notice that while the maximum is significantly lowered, the $H_{c_2}(0)$ reduction observed with increasing $\gamma_{\rm tot}$ is much slower and $H_{c_2}(0)$ for high level of disorder is significantly higher for each value of β.

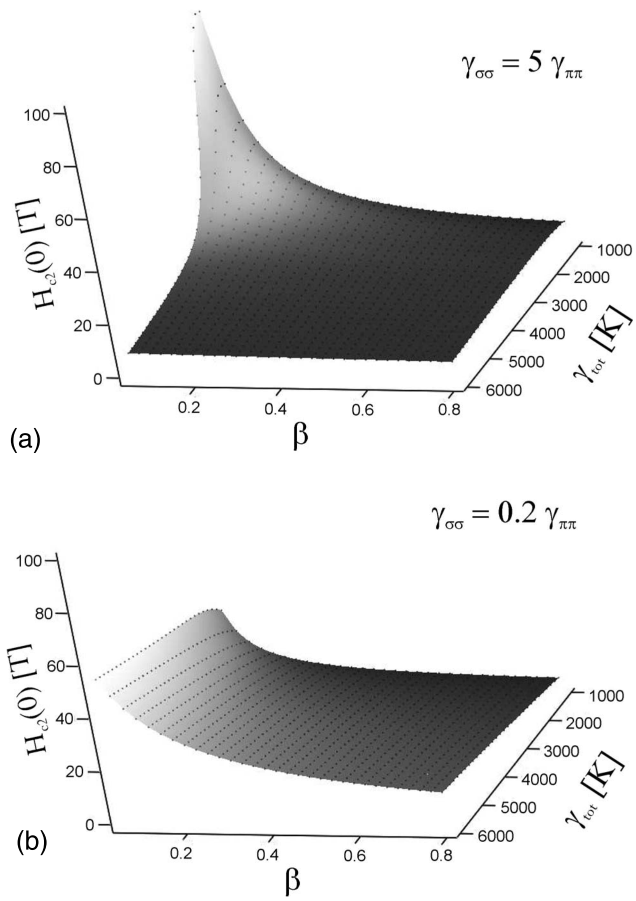

FIG. 3. H_{c_2} as a function of β and γ_{tot} for: (a) $\frac{\gamma_{\sigma\sigma}}{\gamma_{\pi\pi}}=5$ (σ band dirtier than π band) and (b) $\frac{\gamma_{\sigma\sigma}}{\gamma_{\pi\pi}}=0.2$ (π band dirtier than σ band).

These results evidence the primary role in determining H_{c_2} played by the asymmetry of the disorder present in the two bands. This is particularly relevant considering the effects of the smearing of the partial DOS, which are stronger on $N_\sigma(\gamma_{\sigma\sigma})$. In fact when $\gamma_{\sigma\sigma} > \gamma_{\pi\pi}$ the smearing of N_σ reduces more significantly the values of the coupling parameters of MgB_2, then both the critical temperature and the critical field are more rapidly reduced by the introduction of disorder [see the evolution of the surface along the γ_{tot} axis on Fig. 3(a)].

B. Anisotropy of the critical field—γ_H

The primary role played by the σ band evidenced in the previous discussion can be noticed also studying the anisotropy parameter $\gamma_H = \frac{H_{c_2}(\vartheta=\pi/2)}{H_{c_2}(\vartheta=0)}$, which can be evaluated from Eq. (14) for different values of the temperature, of γ_{tot} and $\frac{\gamma_{\sigma\sigma}}{\gamma_{\pi\pi}}$.

In Fig. 4 we show the dependence of $\gamma_H(T=0\ \text{K})$ on γ_{tot} in the case of equal level of disorder in the two bands ($\frac{\gamma_{\sigma\sigma}}{\gamma_{\pi\pi}}=1$), in the case of σ band dirtier than π band ($\frac{\gamma_{\sigma\sigma}}{\gamma_{\pi\pi}}=5$) and in the opposite situation ($\frac{\gamma_{\sigma\sigma}}{\gamma_{\pi\pi}}=0.2$). Observing the plot we can notice that in all cases the anisotropy is reduced with increasing γ_{tot} but when $\gamma_{\sigma\sigma} \gg \gamma_{\pi\pi}$ this effect is much stronger and the anisotropy can be totally eliminated by the introduction of a small amount of disorder in the system. Instead, in the opposite case ($\gamma_{\sigma\sigma} \ll \gamma_{\pi\pi}$) the anisotropy remains around 3 also at the largest level of disorder.

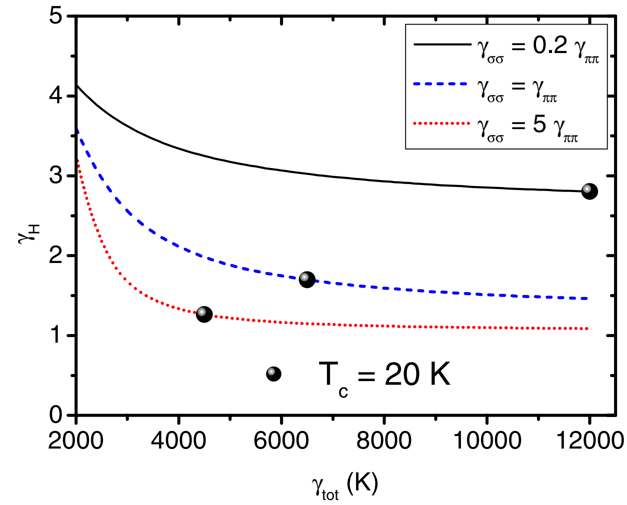

FIG. 4. (Color online) $\gamma_H(0\ K)$ vs γ_{tot}—The three curves represent the case of $\gamma_{\sigma\sigma}=0.2\gamma_{\pi\pi}$ (black solid curve), $\gamma_{\sigma\sigma}=\gamma_{\pi\pi}$ (blue dashed curve) and $\gamma_{\sigma\sigma}=5\gamma_{\pi\pi}$ (red dotted curve). The round symbols correspond to $T_c \approx 20$ K.

The symbols in Fig. 4 mark, on each line, the value of γ_{tot} necessary to get $T_c \approx 20$ K. As a consequence of the smearing of the partial DOS, which depend separately on the single parameters $\gamma_{\sigma\sigma}$ and $\gamma_{\pi\pi}$, very different values of γ_{tot} give the same T_c. In particular, the value of 20 K is obtained by the couples of parameters: $\gamma_{\sigma\sigma} \simeq 3500$ K $\gamma_{\pi\pi} \simeq 700$ K; $\gamma_{\sigma\sigma} = \gamma_{\pi\pi} \simeq 3200$ K; and $\gamma_{\sigma\sigma} \simeq 2000$ K $\gamma_{\pi\pi} \simeq 10\,000$ K.

These values make it clear the main role of $\gamma_{\sigma\sigma}$ in determining T_c. This can be understood considering that T_c is mainly determined by the largest coupling constant $\lambda_{\sigma\sigma}$, which scales with $N_\sigma(\gamma_{\sigma\sigma})$, which in turns is much more affected than N_π by the finite lifetime of carriers.[15]

To explain the fast suppression of anisotropy with increasing impurities in the case of $\gamma_{\sigma\sigma} \gg \gamma_{\pi\pi}$ three main effects can be considered: (i) the increase in interband scattering mechanisms which mixes anisotropic σ and isotropic π carriers; (ii) the increase in isotropic intraband scattering in anisotropic σ band; (iii) the reduction in N_σ and thus of $\lambda_{\sigma\sigma}$, without any reduction in $\lambda_{\pi\pi}$. From a formal point of view the first two mechanisms make the $\hat{A}(n)$ matrix less sensitive to the angular dependence expressed by the κ_σ parameter [see Eq. (11)] and the third one tends to equalize the diagonal terms of $\hat{\Lambda}$ matrix [see Eq. (8)]. In the case $\gamma_{\pi\pi} \gg \gamma_{\sigma\sigma}$ only interband scattering mechanisms (which within our approach scales with γ_{tot}) are effective in reducing the anisotropy but this mechanism comes out much less effective than intraband σ-σ scattering on the $\hat{A}(n)$ matrix. As a consequence of this the anisotropy diminishes rather slowly with increasing disorder.

In any case, looking at the plots we see that the measured value of the anisotropy of the critical field provides a criterion to evaluate the level of disorder present in the single bands. In fact for samples with T_c around 20 K if the anisotropy is larger than 2 ($\gamma_H > 2$) π band is dirtier than σ band; if the anisotropy is nearly suppressed σ band is dirtier than π band.

IV. COMPARISON WITH EXPERIMENTS

In the previous sections we introduced the parameters which determine the upper critical-field value of MgB_2 in the presence of disorder. Now we will show how our self-consistent model allows to establish some general results on the nature and the role of disorder in superconducting MgB_2 by the comparison with experimental data of irradiated samples. To understand this we consider Eq. (14).

We notice that when T and ϑ [and then $\beta(\vartheta)$] are fixed by the experimental conditions, H_{c_2} is determined by the values of $\gamma_{tot} \simeq \gamma_{\sigma\sigma} + \gamma_{\pi\pi}$ and the ratio $\frac{\gamma_{\sigma\sigma}}{\gamma_{\pi\pi}}$ but at the same time also T_c is related to γ_{tot} and $\frac{\gamma_{\sigma\sigma}}{\gamma_{\pi\pi}}$ and this introduces a severe constraint. Indeed, in irradiated MgB_2 a universal T_c vs ρ_0 behavior has been evidenced[14] and this allows to define a T_c vs γ_{tot} curve once the ratio $\frac{\gamma_{\sigma\sigma}}{\gamma_{\pi\pi}}$ has been fixed. At low level of disorder (where the effects of the smearing of partial DOS are negligible) T_c is independent of intraband scattering rates (and thus also of their ratio) and we can safely assume $\gamma_{\sigma\sigma} \simeq \gamma_{\pi\pi}$ (see below). In this regime, T_c depends only on the interband scattering rate which is assumed to be proportional to γ_{tot} [$\gamma_{\sigma\pi} = a\gamma_{tot}$ with $a = 0.067$ (Ref. 22)]. Thus, considering the theoretical expectation for T_c vs $\gamma_{\sigma\pi}$ it is possible to determine γ_{tot} from the measured T_c and the only free variable $\frac{\gamma_{\sigma\sigma}}{\gamma_{\pi\pi}}$ is left in Eq. (14) to fit $H_{c_2}(T)$. At high level of disorder T_c becomes independent of interband scattering rate which makes T_c saturating and intraband mechanisms become dominant. In this regime, T_c is determined by both the parameters γ_{tot} and the ratio $\frac{\gamma_{\sigma\sigma}}{\gamma_{\pi\pi}}$ and this occurs in a nontrivial way because, as discussed above, the partial DOS N_σ and N_π depend in different ways on the intraband scattering rates. Therefore at high level of disorder the values of γ_{tot} and of $\frac{\gamma_{\sigma\sigma}}{\gamma_{\pi\pi}}$ are determined by both the experimental T_c and $H_{c_2}(T)$.

In Fig. 5 we report the comparison between the results of our theoretical model and the critical-field measurements on MgB_2 thin films irradiated with α particles,[23] for the case of applied field parallel to the *ab* plane (we choose this direction because even small disorientation of the film affects the evaluation of H_{c_2} parallel to c axis). The plots show that our model describes with a good accuracy the experiments, and it is able to catch both the change in the slope and the change in the curvature of the phase diagram.

The values of the fitting parameters for each theoretical curve are reported in Table I. For all the samples analyzed we obtain $\gamma_{\sigma\sigma} > \gamma_{\pi\pi}$ and the ratio increases with increasing γ_{tot} (decreasing T_c). This result needs to be compared with different experimental evaluations of intraband scattering rates in irradiated samples. In particular, the analysis of normal-state magnetoresistivity allows a separate evaluation of $\gamma_{\sigma\sigma}$ and $\gamma_{\pi\pi}$.[24,25] These measurements show that indeed unirradiated thin films usually exhibit cleaner σ band while the irradiation makes σ scattering rate progressively higher whereas π scattering rate is less affected. The inset of Fig. 6 shows $\frac{\gamma_{\sigma\sigma}}{\gamma_{\pi\pi}}$ given in Table I as a function of γ_{tot}. The values estimated by magnetoresistivity measurements[24,25] are also reported. A roughly linear behavior is clearly seen. Moreover, we notice that in the limit of small γ_{tot}, $\frac{\gamma_{\sigma\sigma}}{\gamma_{\pi\pi}}$ tends to 1.

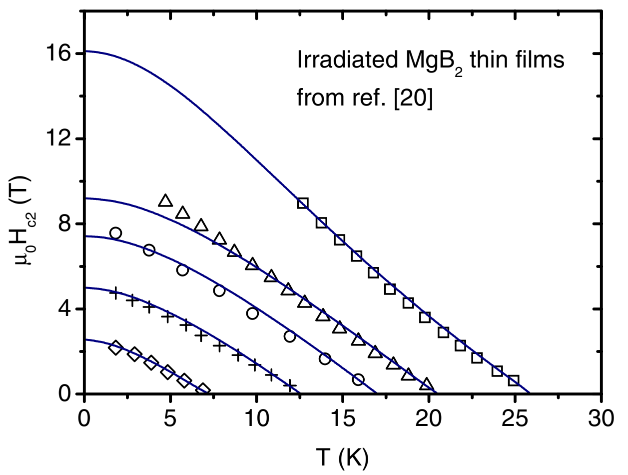

FIG. 5. (Color online) Comparison of the results of our calculation (continuous lines) with measured values of upper critical field parallel to the *ab* plane ($\vartheta = \frac{\pi}{2}$) on oriented thin films disordered with α-particle irradiation. In order to preserve the validity of the approximations adopted in the theoretical calculations we focus our attention on samples with $T_c < 26$ K, which we can assume to be in the dirty limit.

These results imply that defects produced by irradiation (atoms displacements) affect mainly the σ band. This can be understood considering that light B atoms are more easily displaced after interaction with particles than heavier Mg atoms. As the two-dimensional σ orbitals are confined in B planes, the relaxation rate of σ band carriers is more affected than that of delocalized three-dimensional π bands by strongly defected B planes.

Assuming the linear relationship between $\frac{\gamma_{\sigma\sigma}}{\gamma_{\pi\pi}}$ and γ_{tot} reported in the inset of Fig. 6, $H_{c_2}(0)$ as a function of T_c can be calculated. This is reported in Fig. 6 as a continuous line. We notice that starting from high-T_c values (close to the clean limit), with increasing the level of disorder (and thus decreasing T_c) $H_{c_2}(0)$ increases, reaches a maximum (for $T_c \sim 31$ K) and finally it monotonically decreases with decreasing T_c. This behavior has been indeed observed in disordered

TABLE I. The measured values of T_c and the evaluated values of γ_{tot} and $\frac{\gamma_{\sigma\sigma}}{\gamma_{\pi\pi}}$ for the samples analyzed. Symbols refer to Fig. 5.

Symbol	T_c (K)	γ_{tot} (K)	$\frac{\gamma_{\sigma\sigma}}{\gamma_{\pi\pi}}$
□□	26	2800	4.8
△△	20.5	4400	5.6
○○	17	5500	5.9
++	12.5	7300	7.7
◇ ◇	7.5	12000	14

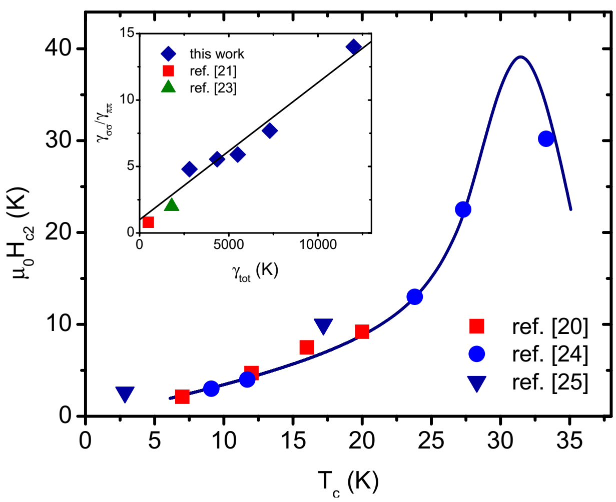

FIG. 6. (Color online) $H_{c_2}(0\ \mathrm{K})$ vs T_c (field parallel to the *ab* plane). In the inset the relationship between γ_{tot} and $\frac{\gamma_{\sigma\sigma}}{\gamma_{\pi\pi}}$ obtained by the fit values in Table I. Values estimated by magnetoresistivity measurements in Refs. 24 and 25 are also reported; in these cases the values of γ_{ii} are defined as $\gamma_{ii}=\gamma_{ii}^{irr}-\gamma_{ii}^{unirr}$, where $\gamma_{ii}^{irr(unirr)}$ is the scattering rate of the *i*th band for the irradiated (unirradiated) sample).

MgB_2.[14,26] For a quantitative comparison we report only experimental data on rather heavily irradiated MgB_2 samples so that they can be safely considered in the dirty limit.[23,26,27] Moreover the extrapolation of $H_{c_2}(0)$ is more reliable when data are available also for temperature close to 0 K. The agreement is quite good.

Another quantity which can be compared with experimental data is the upper critical-field anisotropy γ_H. In Fig. 7 γ_H calculated for $T=0.7T_c$ is reported and compared with experimental data on irradiated samples.[23,27,28] In the calculation of γ_H the same linear relationship between $\frac{\gamma_{\sigma\sigma}}{\gamma_{\pi\pi}}$ and γ_{tot} previously obtained is assumed. As discussed in the previous section, since γ_H is strongly dependent on the ratio $\frac{\gamma_{\sigma\sigma}}{\gamma_{\pi\pi}}$, this is a good test of our model. In the light of this consideration the agreement with the experimental data is very satisfactory.

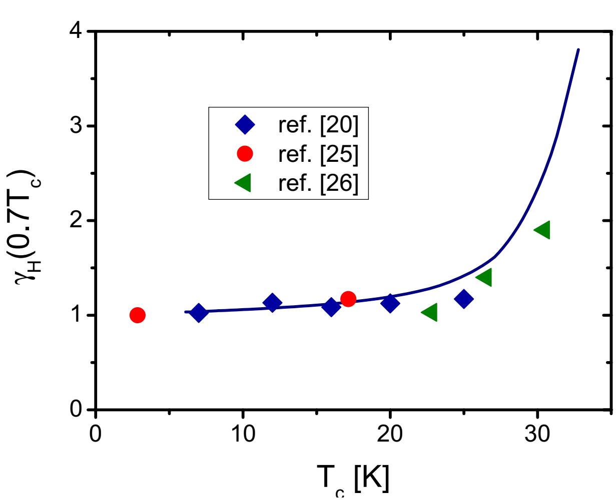

FIG. 7. (Color online) The anisotropy parameter γ_H evaluated at $T=70\%T_c$.

The results shown in Figs. 5–7 demonstrate that, within the considered assumptions (dirty limit, undoped samples), our model reproduces quite well the behaviors experimentally observed. Interestingly, the considered series of data are obtained with different irradiation techniques (i.e., particles, fast neutrons, and thermal neutrons). This implies a universal nature of disorder introduced by irradiation: this had already been suggested by the T_c vs ρ_0 curve but now it emerges more clearly. Our results make it clear that irradiation produces a unique kind of disorder, mainly localized in B planes, thus affecting mainly σ band carriers. In the light of this result we come back to the T_c vs ρ_0 relationship. It was remarked[14] that in MgB_2, in comparison with single band superconductors like A15 materials, T_c is suppressed at a rather low ρ_0 values if compared with saturation resistivity. This means that the superconductivity is suppressed when the mean-free path is still much longer than the interatomic distance. Now we know that defects produced by irradiation mainly affect σ band. Thus resistivity dominated by the more conducting π band assumes rather low values, whereas T_c is suppressed by the strong disorder affecting the σ band. Indeed, looking at Table I, for the samples with T_c=7.5 K, $\gamma_{\sigma\sigma}\simeq 11\,000$ K. Assuming the Fermi velocity of σ band $v_{F_\sigma}\simeq 6.3\times10^5$ m/s (Ref. 20) we evaluate the mean-free path of σ band around 4.3 Å, close the interatomic distance. This nicely explains the apparent inconsistency between the behaviors of MgB_2 and A15 superconductors. On the other hand such very low mean-free path indicates that the system may be so heavily affected by disorder that the same approach is no longer applicable for its description. Indeed, as emphasized in Ref. 15, in presence of extreme disorder (mean-free path comparable with interlayer distance) one cannot neglect Anderson localization effects, which increase the effective Coulomb repulsion[29] and changes in the phonon modes,[30] making the dependence of partial DOS on the relaxation rates unreliable.

V. CONCLUSIONS

We investigated the effects of impurities on the upper critical fields of MgB_2 taking into account the effects of interband and intraband scattering mechanisms. In MgB_2 the former mechanism is negligible with respect to the latter but mixing σ and π Cooper pairs has the crucial role of reducing T_c. Intraband mechanisms have the role of reducing the carrier diffusivities; in addition, within our approach, they cause also a smearing of DOS, reducing the coupling parameters and thus T_c. The inclusion of this additional effect, not considered before, allows for a self-consistent analysis of the experimental data and for an evaluation of the intraband scattering rates of each band. For artificially disordered samples we found that irradiation affects mainly the σ band and the ratio $\gamma_{\sigma\sigma}/\gamma_{\pi\pi}$ increases progressively with increasing doses. This explains well why the anisotropy γ_H of irradiated samples is quickly suppressed even at low level of irradiation.[28] Indeed, within our model, the increase in $\gamma_{\sigma\sigma}$ reduces the anisotropy much more effectively than the increase in $\gamma_{\pi\pi}$. Moreover a dirtier σ band rationalizes why in MgB_2 T_c is completely suppressed at rather low-resistivity values in comparison with other superconductors.[14] In fact for very dirty σ band and rather clean π band, resistivity values, determined by the most conducting π band, remain rather low, whereas T_c comes out suppressed by a significant reduction in the partial σ DOS.

As regards the upper critical field, our analysis makes it clear that the increase in $\gamma_{\sigma\sigma}$ has the twofold and antithetic effects of decreasing the coherence length (which increases H_{c_2}) and of producing a smearing of the σ DOS (which reduces T_c and thus H_{c_2}). Indeed, one of the main outcomes of this work is the prediction that in order to increase H_{c_2}, it would be more performing to introduce a kind of disorder which affects selectively the π bands, being the π DOS and consequently T_c less affected by the smearing. As regards thin films, huge H_{c_2} values, close to the paramagnetic limit, were observed in samples in which an anomalous upward curvature of H_{c_2} parallel to c axis was also observed,[8,9] which is another evidence of dirtier π band.[10,13] Unfortunately the nature of disorder present in thin films has not yet been reproduced in bulk materials which would be more suitable for high-field applications. In bulk samples, in order to include impurities which mainly affect π carriers, Mg was substituted with Al,[31,32] but, actually, Al substitution also dopes the systems, thus emptying the σ bands and strongly reducing T_c.[33] A better candidate for increasing H_{c_2} without suppressing T_c might be the substitution of Mg with Li, which affects negligibly the electronic structure.[34,35] This was indeed tried[36,37] but the amount of impurities that were included was not enough to carry the system in the dirty limit. Now that the physical reasons for which dirtier π band may improve significantly the performance of MgB_2 are better understood, we wish such investigations could proceed more quickly.

ACKNOWLEDGMENTS

This work is supported by MIUR under Project No. PRIN2006021741 and by the Compagnia di S Paolo. The authors acknowledge A. Gurevich for useful scientific discussion.

DERIVATION OF Hc_2 DEPENDENCE ON THE PARAMETERS OF Eq. (14)

To obtain the expression for the upper critical field H_{c_2} we start from Eq. (10) that we write in the form

$$\hat{M}\bar{\mathbf{\Delta}} = 0$$

with

$$\hat{M} = \hat{\Lambda}^{-1} - \pi T \sum_{|\omega_m|<\omega_c} \hat{A}^{-1}(m).$$

In order to determine the conditions on magnetic field and temperature for the transition of the system from normal to superconducting phase we set to zero the determinant of the matrix $\hat{M}$.

From Eq. (13) we obtain

$$[\hat{A}(n)]^{-1} = \frac{1}{\mathrm{Det}(n)}\begin{pmatrix} |\omega_n|(1+\Lambda_\pi) + \alpha_\pi\xi_\pi + \frac{\gamma_{\pi\sigma}}{2} & \frac{\gamma_{\sigma\pi}}{2} \\ \frac{\gamma_{\pi\sigma}}{2} & |\omega_n|(1+\Lambda_\sigma) + \kappa_\sigma\alpha_\sigma\xi_\sigma + \frac{\gamma_{\sigma\pi}}{2} \end{pmatrix}$$

with

$$\Lambda_i = \sum_j \lambda_{ij},$$

$$\xi_i = \frac{1}{3/2(\gamma_{ii}+\gamma_{ij})}. \tag{A1}$$

Here Det(n) is the determinant of $\hat{A}(n)$

$$\mathrm{Det}(n) = a(|\omega_n| - \omega_1)(|\omega_n| - \omega_2),$$

where $a=(1+\Lambda_\sigma)(1+\Lambda_\pi)$ and ω_1,ω_2 are the roots of the equation

$$\mathrm{Det}[\hat{A}(n)] = 0.$$

Introducing the matrices

$$\hat{\Lambda} = \begin{pmatrix} 1+\Lambda_\pi & 0 \\ 0 & 1+\Lambda_\sigma \end{pmatrix},$$

$$\hat{\eta}_1 = \frac{1}{2}\begin{pmatrix} \gamma_{\pi\sigma} & \gamma_{\sigma\pi} \\ \gamma_{\pi\sigma} & \gamma_{\sigma\pi} \end{pmatrix},$$

$$\hat{\eta}_2 = \begin{pmatrix} \alpha_\pi\xi_\pi & 0 \\ 0 & \kappa_\sigma\alpha_\sigma\xi_\sigma \end{pmatrix}, \tag{A2}$$

we obtain that $\hat{M}$ can be written in the form

$$\hat{M} = \hat{\Lambda}^{-1} - L_1(T)\hat{\Lambda} + L_2(T)[\hat{\eta}_1 + \hat{\eta}_2], \tag{A3}$$

where the functions $L_1(T)$ and $L_2(T)$ in Eq. (A3) are defined as

$$L_1(T) = \frac{\pi T}{a} \sum_{|\omega_m|<\omega_c} \frac{|\omega_m|}{[|\omega_m| - \omega_1][|\omega_m| - \omega_2]},$$

$$L_1(T) = \frac{\pi T}{a} \sum_{|\omega_m|<\omega_c} \frac{1}{[|\omega_m| - \omega_1][|\omega_m| - \omega_2]}.$$

In terms of the digamma function $\psi(z)$, $L_1(T)$, and $L_2(T)$ take the form

$$L_1(T) = \frac{\omega_1}{a(\omega_1 - \omega_2)}\left[\psi\left(\frac{\omega_c - \omega_1}{2\pi T} + 1\right) - \psi\left(-\frac{\omega_1}{2\pi T} + \frac{1}{2}\right)\right] - \frac{\omega_2}{a(\omega_1 - \omega_2)} \times \left[\psi\left(\frac{\omega_c - \omega_2}{2\pi T} + 1\right) - \psi\left(-\frac{\omega_2}{2\pi T} + \frac{1}{2}\right)\right],$$

$$L_2(T) = \frac{1}{a(\omega_1 - \omega_2)}\left[\psi\left(\frac{\omega_c - \omega_1}{2\pi T} + 1\right) - \psi\left(-\frac{\omega_1}{2\pi T} + \frac{1}{2}\right)\right] - \frac{1}{a(\omega_1 - \omega_2)}\left[\psi\left(\frac{\omega_c - \omega_2}{2\pi T} + 1\right) - \psi\left(-\frac{\omega_2}{2\pi T} + \frac{1}{2}\right)\right].$$

Assuming a linear relationship between the total scattering rate and the $\sigma\pi$ interband scattering rate $\gamma_{\sigma\pi}=a\gamma_{\text{tot}}$ and defining the parameter $k=\frac{\gamma_{\sigma\sigma}}{\gamma_{\pi\pi}}$, whose value indicates which is the dirtier band in the system, we can express all the parameters relative to the scattering with impurities in terms of k and γ_{tot}, and, in particular, we have for the quantities ξ_i defined in Eq. (A1),

$$\xi_\sigma(\gamma_{\text{tot}},k) = \left[\frac{3}{2}\gamma_{\text{tot}}\left(a + \frac{k}{k+1}\right)\right]^{-1},$$

$$\xi_\pi(\gamma_{\text{tot}},k) = \left[\frac{3}{2}\gamma_{\text{tot}}\left(a\frac{N_\sigma}{N_\pi} + \frac{1}{k+1}\right)\right]^{-1}.$$

Moreover introducing the parameter $\beta(\vartheta)$ defined in Eq. (15) we can write the matrix in Eq. (A2) in the form

$$\hat{\eta}_2 = \alpha_\pi \begin{pmatrix} \xi_\pi & 0 \\ 0 & \beta(\vartheta)\xi_\sigma \end{pmatrix},$$

where $\alpha_\pi=\frac{e}{2}H_{c_2}(v_{F_\pi}^{ab})^2$ contains the dependence on magnetic field.

In this way we have expressed the dependence of H_{c_2} in terms of the set of parameters which appear in Eq. (14).

[1] J. Nagamatsu, N. Nakagawa, T. Muranaka, Y. Zenitani, and J. Akimitsu, Nature (London) **410**, 63 (2001).

[2] H. Suhl, B. T. Matthias, and L. R. Walker, Phys. Rev. Lett. **3**, 552 (1959).

[3] S. Patnaik, L. D. Cooley, A. Gurevich, A. A. Polyanskii, J. Jiang, X. Y. Cai, A. A. Squitieri, M. T. Naus, M. K. Lee, J. H. Choi, L. Belenky, S. D. Bu, J. Letteri, X. Song, D. G. Schlom, S. E. Babcock, C. B. Eom, E. E. Hellstrom, and D. C. Larbalestier, Supercond. Sci. Technol. **14**, 315 (2001).

[4] C. B. Eom, M. K. Lee, J. H. Choi, L. J. Belenky, X. Song, L. D. Cooley, M. T. Naus, S. Patnaik, J. Jiang, M. Rikel, A. Polyanskii, A. Gurevich, and X. Y. Cai, Nature (London) **411**, 558 (2001).

[5] V. Ferrando, P. Manfrinetti, D. Marré, M. Putti, I. Sheikin, C. Tarantini, and C. Ferdeghini, Phys. Rev. B **68**, 094517 (2003).

[6] F. Bouquet, R. A. Fisher, N. E. Philips, D. G. Hinks, and J. D. Jorgensen, Phys. Rev. Lett. **87**, 047001 (2001).

[7] E. Ohmichi, E. Komatsu, T. Masui, S. Lee, S. Tajima, and T. Osada, Phys. Rev. B **70**, 174513 (2004).

[8] A. Gurevich, S. Patnaik, V. Braccini, K. H. Kim, C. Mielke, X. Song, L. D. Cooley, S. D. Bu, D. M. Kim, J. H. Choi, L. J. Belenky, J. Giencke, M. K. Lee, W. Tian, X. Q. Pan, A. Siri, E. E. Hellstrom, C. B. Eom, and D. C. Larbalestier, Supercond. Sci. Technol. **17**, 278 (2004).

[9] V. Braccini, A. Gurevich, J. E. Giencke, M. C. Jewell, C. B. Eom, D. C. Larbalestier, A. Pogrebnyakov, Y. Cui, B. T. Liu, Y. F. Hu, J. M. Redwing, Qi Li, X. X. Xi, R. K. Singh, R. Gandikota, J. Kim, B. Wilkens, N. Newman, J. Rowell, B. Moeckly, V. Ferrando, C. Tarantini, D. Marré, M. Putti, C. Ferdeghini, R. Vaglio, and E. Haanappel, Phys. Rev. B **71**, 012504 (2005).

[10] A. Gurevich, Phys. Rev. B **67**, 184515 (2003).

[11] A. A. Golubov and A. E. Koshelev, Phys. Rev. B **68**, 104503 (2003).

[12] M. Mansor and J. P. Carbotte, Phys. Rev. B **72**, 024538 (2005).

[13] A. Gurevich, Physica C **456**, 160 (2007).

[14] M. Putti, R. Vaglio, and J. M. Rowell, Supercond. Sci. Technol. **21**, 043001 (2008).

[15] M. Putti, P. Brotto, M. Monni, E. Galleani d'Agliano, A. Sanna, and S. Massidda, EPL **77**, 57005 (2007).

[16] M. Prohammer and J. P. Carbotte, Phys. Rev. B **42**, 2032 (1990).

[17] P. B. Allen and B. Mitrović, *Solid State Physics*, edited by H. Ehrenreich, F. Seitz, and D. Turnbull (Academic, New York, 1982), Vol. 37.

[18] A. A. Golubov, J. Kortus, O. V. Dolgov, O. Jepsen, Y. Kong, O. K. Andersen, B. J. Gibson, K. Ahn, and R. K. Kremer, J. Phys.: Condens. Matter **14**, 1353 (2002).

[19] G. A. Ummarino, D. Daghero, R. S. Gonnelli, and A. H. Moudden, Phys. Rev. B **71**, 134511 (2005).

[20] A. Brinkman, A. A. Golubov, H. Rogalla, O. V. Dolgov, J. Kortus, Y. Kong, O. Jepsen, and O. K. Andersen, Phys. Rev. B **65**, 180517 (2002) R.

[21] M. Putti, M. Affronte, C. Ferdeghini, P. Manfrinetti, C. Tarantini, and E. Lehmann, Phys. Rev. Lett. **96**, 077003 (2006).

[22] Actually in Ref. 15 a slightly different value of $a=0.059$ was given. This discrepancy is due to the fact that the resistivity has been normalized following the criterion given in Ref. 14 which fixed $\rho(300\ \text{K})-\rho(40\ \text{K})=7.5\ \mu\Omega$ cm.

[23] R. Gandikota, R. K. Singh, J. Kim, B. Wilkens, N. Newman, J. M. Rowell, A. V. Pogrebnyakov, X. X. Xi, J. M. Redwing, S. Y. Xu, Q. Li, and B. H. Moeckly, Appl. Phys. Lett. **87**, 072507 (2005).

[24] M. Monni, I. Pallecchi, C. Ferdeghini, V. Ferrando, A. Floris, E.

Galleani D'Agliano, E. Lehmann, I. Sheikin, C. Tarantini, X. X. Xi, S. Massidda, and M. Putti, EPL **81**, 67006 (2008).

[25] I. Pallecchi, V. Ferrando, E. Galleani D'Agliano, D. Marré, M. Monni, M. Putti, C. Tarantini, F. Gatti, H. U. Aebersold, E. Lehmann, X. X. Xi, E. G. Haanappel, and C. Ferdeghini, Phys. Rev. B **72**, 184512 (2005).

[26] C. Tarantini, H. U. Aebersold, V. Braccini, G. Celentano, C. Ferdeghini, V. Ferrando, U. Gambardella, F. Gatti, E. Lehmann, P. Manfrinetti, D. Marré, A. Palenzona, I. Pallecchi, I. Sheikin, A. S. Siri, and M. Putti, Phys. Rev. B **73**, 134518 (2006).

[27] V. Ferrando, I. Pallecchi, C. Tarantini, D. Marré, M. Putti, C. Ferdeghini, F. Gatti, H. U. Aebersold, E. Lehmann, E. Haanappel, I. Sheikin, P. Orgiani, and X. X. Xi, J. Appl. Phys. **101**, 043903 (2007).

[28] C. Krutzler, M. Zehetmayer, M. Eisterer, H. W. Weber, N. D. Zhigadlo, and J. Karpinski, Phys. Rev. B **75**, 224510 (2007).

[29] P. W. Anderson, K. A. Muttalib, and T. V. Ramakrishnan, Phys. Rev. B **28**, 117 (1983).

[30] D. Di Castro, E. Cappelluti, M. Lavagnini, A. Sacchetti, A. Palenzona, M. Putti, and P. Postorino, Phys. Rev. B **74**, 100505 (2006) R.

[31] M. Putti, C. Ferdeghini, M. Monni, I. Pallecchi, C. Tarantini, P. Manfrinetti, A. Palenzona, D. Daghero, R. S. Gonnelli, and V. A. Stepanov, Phys. Rev. B **71**, 144505 (2005).

[32] J. Karpinski, N. D. Zhigadlo, G. Schuck, S. M. Kazakov, B. Batlogg, K. Rogacki, R. Puzniak, J. Jun, E. Müller, P. Wägli, R. Gonnelli, D. Daghero, G. A. Ummarino, and V. A. Stepanov, Phys. Rev. B **71**, 174506 (2005).

[33] J. Kortus, O. V. Dolgov, R. K. Kremer, and A. A. Golubov, Phys. Rev. Lett. **94**, 027002 (2005).

[34] M. Monni, C. Ferdeghini, M. Putti, P. Manfrinetti, A. Palenzona, M. Affronte, P. Postorino, M. Lavagnini, A. Sacchetti, D. Di Castro, F. Sacchetti, C. Petrillo, and A. Orecchini, Phys. Rev. B **73**, 214508 (2006).

[35] F. Bernardini and S. Massidda, Phys. Rev. B **74**, 014513 (2006).

[36] J. Karpinski, N. D. Zhigadlo, S. Katrych, K. Rogacki, B. Batlogg, M. Tortello, and R. Puzniak, Phys. Rev. B **77**, 214507 (2008).

[37] I. Pallecchi, P. Brotto, C. Ferdeghini, M. Putti, A. Palenzona, P. Manfrinetti, A. Geddo Lehmann, A. Orecchini, C. Petrillo, F. Sacchetti, M. Affronte, G. Allodi, R. De Renzi, S. Serventi, A. Andreone, G. Lamura, D. Daghero, R. S. Gonnelli, and M. Tortello, Supercond. Sci. Technol. **22**, 095014 (2009).